Journal of Renewable and Sustainable Energy

RESEARCH ARTICLE | FEBRUARY 18 2026

Quantum algorithm-enhanced evaluation method for hybrid wind-PV system projects considering carbon trading

Zhanpeng Xu; Zhehan Li; Longze Wang; Shizhao Wang; Yuteng Mao; Zhenhao Weng; Yan Zhang; Zihan Xie; Meicheng Li

Check for updates

J. Renewable Sustainable Energy 18, 016314 (2026)
https://doi.org/10.1063/5.0306208

View Online
Export Citation

Articles You May Be Interested In

Optimal capacity of variable-speed pumped storage for wind power consumption based on double-layer stochastic programming

J. Renewable Sustainable Energy (April 2023)

Editorial for the collection “Wind tunnel research for renewable energies”

J. Renewable Sustainable Energy (September 2025)

Joint optimization of the number, type and layout of wind turbines for a new offshore wind farm

J. Renewable Sustainable Energy (October 2020)

04 March 2026 02:12:36

AIP Advances
Why Publish With Us?
21DAYS average time to 1st decision
OVER 4 MILLION views in the last year
INCLUSIVE scope
Learn More
AIP Publishing

AIP Publishing

Journal of Renewable and Sustainable Energy ARTICLE pubs.aip.org/aip/rse

Quantum algorithm-enhanced evaluation method for hybrid wind-PV system projects considering carbon trading

Cite as: J. Renewable Sustainable Energy **18**, 016314 (2026); doi: 10.1063/5.0306208
Submitted: 9 October 2025 · Accepted: 3 December 2025 ·
Published Online: 18 February 2026

View Online Export Citation CrossMark

Zhanpeng Xu,[1,a] Zhehan Li,[1,b] Longze Wang,[1,c] Shizhao Wang,[1,d] Yuteng Mao,[1,e] Zhenhao Weng,[1,f] Yan Zhang,[2,3,g] Zihan Xie,[1,h] and Meicheng Li[1,i]

AFFILIATIONS

[1]State Key Laboratory of Alternate Electrical Power System with Renewable Energy Sources, School of New Energy, North China Electric Power University, Beijing 102206, China
[2]School of Economics and Management, North China Electric Power University, Beijing 102206, China
[3]Beijing Key Laboratory of New Energy and Low-Carbon Development, Beijing 102206, China

[a)]Electronic mail: 120222111030@ncepu.edu.cn
[b)]Electronic mail: 120232111033@ncepu.edu.cn
[c)]Electronic mail: lzwang@ncepu.edu.cn
[d)]Electronic mail: 120242211126@ncepu.edu.cn
[e)]Electronic mail: 120232211123@ncepu.edu.cn
[f)]Electronic mail: 120211100525@ncepu.edu.cn
[g)]Electronic mail: zhangyan8698@ncepu.edu.cn
[h)]Electronic mail: 120231020219@ncepu.edu.cn
[i)]Author to whom correspondence should be addressed: mcli@ncepu.edu.cn

ABSTRACT

Hybrid wind–PV system projects (HWPSPs) help increase renewable energy penetration and gain additional advantages under carbon emission trading (CET) mechanisms. However, evolving CET policies and carbon price volatility introduce uncertainty into the objective evaluation of such projects. This study proposes a quantum-enhanced evaluation framework that integrates quantum particle swarm optimization (QPSO) with the technique for order preference by similarity to ideal solution (TOPSIS) to assess HWPSP performance in a carbon-trading context. A CET-integrated evaluation indicator system is first constructed based on an in-depth analysis of CET's influence on HWPSPs. The coupled relationships among indicators are then modeled via quantum superposition and entanglement, while indicator weights are optimized using QPSO. Subsequently, TOPSIS is applied to obtain the final assessment results. A newly constructed HWPSP at a thermal power plant in Beijing, China, is used as a case study to validate the method. The results show that QPSO improves convergence speed by 35.8% compared with classical PSO and enhances robustness, with ranking fluctuations remaining within ±2% under 5%–10% indicator perturbations —vs 8%–12% for traditional linear multi-criteria decision-making (MCDM) methods. Finally, the proposed method is validated using a real HWPSP project at a thermal power plant in Beijing. Incorporating CET reduces the Euclidean distance between the project's comprehensive evaluation score and the ideal scheme by 4.17%, elevating its final ranking to the "Excellent" level.

Published under an exclusive license by AIP Publishing. https://doi.org/10.1063/5.0306208

I. INTRODUCTION

A. Background and motivation

Global climate change has created an urgent demand for clean energy sources.[1] Hybrid wind-PV system projects (HWPSP), characterized by their ability to combine decentralized wind and solar power,[2] have emerged as a key driver in expanding renewable energy's share in the energy mix.[3,4] However, increasing concerns about carbon emissions have added complexity to the evaluation of the sustainability and economic viability of these projects. While carbon trading mechanisms offer enterprises incentives to proactively reduce their carbon footprint,[5,6] accurately assessing the comprehensive impact of HWPSP in the context of carbon trading remains a complex and unresolved

04 March 2026 02:12:36

Published under an exclusive license by AIP Publishing

challenge. Conventional evaluation methods do not fully account for the dynamic influence of carbon trading on these projects[7] and are inadequate in providing decision-making support amid market fluctuations.[8,9] Thus, there is a pressing need for a novel assessment methodology that can thoroughly and accurately evaluate the feasibility of HWPSP while incorporating the true implications of carbon trading.

B. Literature review

1. HWPSP based on CET

The background of carbon emissions trading (CET) can be traced back to international climate change agreements under the United Nations Framework Convention on Climate Change, such as the Kyoto Protocol (1997) and the Paris Agreement (2015).[10,11] Existing research on power generation enterprises primarily focuses on factors influencing carbon emissions, market mechanisms, policy effects, and related aspects. Among these enterprises, thermal power plants are identified as the largest contributors to carbon dioxide emissions.[12] Some scholars have utilized differential models to investigate the impact of CET systems on the environmental performance of power plants. Their findings suggest that incorporating carbon taxes into the carbon trading market can incentivize power companies to adopt green transformations.[13] In Ref. 14, the authors analyzed CET data from 2008 to 2012, focusing on the European Union's mature CET market. They highlighted that carbon prices are influenced not only by domestic economic factors but also by international environmental factors. Furthermore, Gavard and Kirat[15] discovered that energy prices and European allowances prices significantly impact carbon prices. In Ref. 16 the authors compared the accuracy of various computational models in predicting carbon prices, concluding that hybrid fuzzy neural networks provided the most accurate predictions, offering valuable insights for risk management in carbon trading. Similarly, in Ref. 17, the authors employed economic forecasting and policy analysis models to study the relationship between emissions trading mechanisms and the benefits of emission reductions in the Chinese power sector. In Ref. 18 a P2P trading model was constructed, improving both economic and environmental benefits through innovative mechanisms. The study introduced blockchain cross-chain interoperability technology into the real-time data-sharing network for electricity and carbon co-trading, providing a reference for the real-time integration of electricity and carbon markets. In Ref. 19, the authors quantitatively evaluated low-carbon energy transition policies, focusing on policy intensity, objectives, and tools. Using ridge regression models, the study analyzed the carbon reduction effects of these policies and proposed relevant recommendations for reducing carbon emissions.

HWPSP has recently emerged as a key development in the renewable energy landscape. These systems integrate wind and PV power generation within industrial premises to harness wind and solar energy, thereby simultaneously meeting electricity demands and reducing carbon emissions.[20] However, the development of HWPSP is currently influenced by factors such as subsidy policies and electricity price adjustments.[21] In response to these challenges,[22] considered user preferences and characteristics, constructing a game model for the PV supply chain under different power structures. The study explored optimal decisions for PV supply chain enterprises and government subsidy policies. Recent studies have explored the hybridization of wind and solar systems to optimize renewable energy output. In Ref. 23 the authors evaluated capacity allocation strategies for stand-alone hybrid systems, highlighting the advantages of genetic algorithms over traditional methods. They also analyzed the wind-solar capacity ratio from the perspectives of policy compliance and land-use impact, proposing that minimizing the coefficient of variation is essential for determining the optimal wind-to-solar ratio to reduce energy variability, particularly in regions with land constraints and in China. In parallel, Xu *et al.*[24] used a quasi-experimental method, propensity score matching difference-in-differences (PSM-DID), to examine the impact of PV poverty alleviation projects on local economies, based on panel data from 852 provinces and 12 counties in China. Their study proposed sustainable strategies for PV poverty alleviation projects through enhanced regional collaboration. In addition to these studies, researchers have explored various aspects of distributed HWPSP, including site selection,[25,26] PV component layout,[27,28] system design,[29] grid integration,[30] as well as broader topics like technological advancements,[31,32] energy management,[33,34] and performance optimization.[35] Existing studies on HWPSPs have primarily focused on technical optimization, economic feasibility, and environmental benefits. Many works analyze the impact of resource complementarity, system configuration, and operation strategies on project performance. Recent research also considers the policy context of CET, indicating that carbon pricing can significantly influence investment decisions and project profitability. However, most existing studies treat CET as an external economic factor without integrating it into a systematic multi-criteria evaluation framework. In addition, the interaction between carbon reduction benefits and other criteria (such as economic, social, and environmental indicators) is often simplified or ignored, limiting the comprehensiveness of the evaluation results.

2. Comprehensive evaluation method

From the perspective of evaluation methodology, multi-criteria decision-making (MCDM) techniques have gradually become the mainstream tools for assessing renewable and low-carbon energy projects. Classical frameworks such as the analytic hierarchy process (AHP), entropy weighting, TOPSIS, COPRAS, and related hybrid schemes provide a structured way to combine economic, technical, environmental, and social indicators into an integrated score.[36–38] Owing to their clear logic and relatively low data requirements, these methods have been widely applied in project selection, site planning, and policy analysis for conventional power systems as well as emerging renewable energy projects.[39,40] With the growing complexity of decision contexts, a second group of studies has proposed enhanced or hybrid MCDM models. Typical examples include AHP–entropy combinations to balance subjective and objective information,[41] fuzzy extensions of TOPSIS and COPRAS to represent linguistic judgements,[42] and DEA-based formulations to benchmark the relative efficiency of comparable projects.[40] These approaches improve robustness against subjective bias and data uncertainty, thereby offering more nuanced and reliable evaluation outcomes than purely deterministic techniques.[42,43] Despite these advancements, several methodological limitations remain. Most existing MCDM frameworks implicitly assume linear additivity and independence among indicators, limiting their ability to capture the nonlinear coupling typically observed among technical performance, economic returns, and environmental impacts. Moreover, the determination of indicator weights often relies on heuristic or locally optimized procedures, which may lead to

04 March 2026 02:12:36

Published under an exclusive license by AIP Publishing

multiple local optima and reduce the credibility of ranking results.[41,44] In addition, when policy-driven factors such as CET are incorporated, the interdependence between carbon-related indicators and traditional economic or environmental criteria becomes more pronounced, yet conventional MCDM models are not explicitly designed to accommodate such complex interactions.[37,38] These considerations suggest that an effective evaluation framework for hybrid wind–photovoltaic systems under CET should retain the interpretability of MCDM methods while integrating a more powerful global optimization mechanism capable of deriving indicator weights and representing nonlinear relationships among evaluation criteria.

3. Quantum derivative algorithm-QPSO

Quantum computing, first conceptualized by Feynman in the 1980s,[45] has seen rapid advancements in recent years. Unlike classical bits, which exist in binary states (0 or 1), qubits can exist in superposition, representing both states simultaneously. By leveraging superposition, entanglement, and interference, quantum algorithms exhibit inherent parallelism and offer the potential for exponential speedups in solving complex problems. Prominent examples include Shor's algorithm[46] and Grover's algorithm.[47] In 1996, the integration of quantum computing with genetic algorithms was proposed,[48] marking the beginning of quantum swarm intelligence optimization. Subsequently, quantum genetic algorithms were developed,[49] where qubits and quantum rotation gates were introduced to encode and update chromosomes, paving the way for numerous quantum swarm intelligence algorithms over the next two decades.[50–56] These algorithms have since been enhanced with various modifications and applied to a wide range of problems.

Particle swarm optimization (PSO) has also been adapted to the quantum domain, giving rise to the quantum particle swarm optimization (QPSO) algorithm.[51] By integrating quantum mechanics, QPSO harnesses the power of qubit superposition and entanglement, achieving greater search efficiency and robustness compared to classical PSO. QPSO has found applications in diverse fields, such as medical technology,[57,58] chemical engineering,[59,60] and materials science.[61,62] In the field of comprehensive evaluation, classical optimization algorithms such as PSO and genetic algorithms (GA) have demonstrated considerable effectiveness. However, they exhibit inherent limitations: their global search capability is often insufficient to cope with nonlinear and strongly coupled indicators, and their performance is highly sensitive to parameter tuning and initialization. As a result, these methods frequently yield unstable or locally optimal weight solutions, particularly in HWPSP evaluations, where natural, economic, environmental, and carbon-emission-related indicators interact in complex ways. In contrast, quantum optimization methods offer several advantages that directly address these shortcomings. The QPSO algorithm employs probabilistic quantum-state evolution, enabling broader global exploration with fewer heuristic parameters and reduced dependency on initial conditions. This leads to more stable convergence and stronger robustness when handling uncertain or irregular data distributions. Moreover, the population update mechanism in QPSO supports parallel exploration of multiple candidate solutions, thereby improving its ability to maintain consistent weight distributions across diverse data scenarios. These distinctions reveal a clear methodological gap: traditional optimization algorithms struggle to determine accurate weights in high-dimensional, nonlinear, and uncertain energy evaluation problems, whereas QPSO provides a more reliable and theoretically grounded alternative. Despite these strengths, existing applications of QPSO have primarily focused on operational optimization or parameter tuning, with limited attention to MCDM.

Table I summarizes key characteristics of representative evaluation methods. As shown, traditional and hybrid MCDM approaches provide structured decision rules but often rely on subjective or linear weight determination. Quantum-inspired algorithms demonstrate stronger global search capability but have not been effectively combined with MCDM methods for HWPSP evaluation, particularly under carbon trading mechanisms. This gap motivates the present study, which integrates QPSO-based weight determination with

TABLE I. Comparative analysis of representative evaluation methods for renewable-energy project assessment.

Method	Advantages	Limitations	Consider CET?	Nonlinear indicator interaction?
AHP / Entropy	Simple, widely used; good interpretability	Subjective;linear assumptions	✗	✗
Fuzzy MCDM	Handles uncertainty; flexible	Computationally heavy; still relies on expert rules	✗	Partial
COPRAS/ TOPSIS	Efficient;stable ranking	Weights often heuristic; cannot model indicator coupling	✗	✗
Hybrid MCDM (AHP–Entropy, Fuzzy-TOPSIS)	Improved objectivity	Still lacks global search ability; linear criteria	Sometimes	✗
QGA / QBEA	Strong global search ability	Limited applicability; no MCDM integration	✗	✓
QPSO (This study)	Strong global convergence; models indicator coupling; suitable for weight optimization	Requires parameter design	✓	✓

04 March 2026 02:12:36

Published under an exclusive license by AIP Publishing

TOPSIS to construct a comprehensive, policy-aware evaluation framework for HWPSPs.

C. Contributions and article structure

Addressing the research gap in the comprehensive evaluation of HWPSPs under carbon trading mechanisms, this study incorporates CET policy factors and carbon price fluctuations into the assessment framework. We establish a CET-integrated evaluation indicator system, consider the nonlinear coupling among indicators, and adopt a quantum-enhanced optimization approach for weight determination. The effectiveness of the proposed framework is further verified using real project data. The main contributions of this study are as follows:

1. A CET-integrated evaluation indicator system tailored for HWPSPs. A six-dimensional, eighteen-indicator system is constructed to comprehensively represent the economic, environmental, social, technical, resource, and carbon-trading-related characteristics of HWPSPs. Unlike existing frameworks, the proposed system explicitly incorporates CET-driven benefits and risks, allowing a more realistic reflection of project performance under national carbon policies.
2. A quantum-enhanced weight determination method based on QPSO. Compared with classical PSO, QPSO achieves 35.8% faster convergence and exhibits significantly higher robustness, with a variance of optimal solutions of only 0.005 in 20 independent runs (vs. 0.013 for PSO), demonstrating superior global search stability.
3. A QPSO-TOPSIS hybrid evaluation model capable of capturing nonlinear indicator interactions. The model effectively captures nonlinear coupling among the indicators. Under 5%–10% indicator perturbations, the ranking fluctuation remains below 2%, substantially outperforming traditional linear MCDM methods (8%–12%).
4. A real-world case demonstration under different carbon price scenarios. A practical HWPSP project in Beijing is evaluated to validate the effectiveness of the proposed model. Furthermore, sensitivity analysis under varying CET prices is conducted to examine the stability of project rankings, illustrating the importance of carbon pricing in decision-making. The results indicate that incorporating CET significantly improves the project's relative closeness to the ideal scheme.

The remainder of this paper is organized as follows: Sec. II presents the foundational design of HWPSP and outlines the comprehensive evaluation indicator system. Section III introduces the methodology, including the process of weight calculation using the QPSO algorithm and the application of the TOPSIS method for comprehensive evaluation. In Sec. IV, real-world case studies are used to validate the constructed evaluation system and methodology, with detailed weight calculation and evaluation analysis. Finally, Sec. V concludes the research.

II. SYSTEM HARDWARE STRUCTURE

The hardware structure of the HWPSP primarily comprises two subsystems: the PV system and the wind power system, as illustrated in Fig. 1. These subsystems function independently yet are integrated to collaboratively supply energy within industrial facilities or buildings. The wind power system generates AC power, which is rectified into DC using a rectifier, while the PV system produces DC power that is regulated through a converter. Both DC power outputs are then combined and processed through an inverter, where they are converted back into AC for final distribution to various loads, such as factories or commercial buildings. This coordinated design ensures efficient utilization of both wind and solar energy resources, providing a stable and reliable energy supply to meet the facility's demand.

In the HWPSP, the wind power subsystem operates by converting the kinetic energy of wind into mechanical energy, which is subsequently transformed into electrical power. As shown in Fig. 2(a), the system uses a variable pitch wind turbine that adjusts the blade angles to maximize energy capture from changing wind conditions. The kinetic energy of the wind is harnessed and transferred to the turbine, where it is converted into mechanical energy by the rotor and then into electrical energy by the generator. The system dynamically controls the turbine's movement to optimize efficiency while maintaining

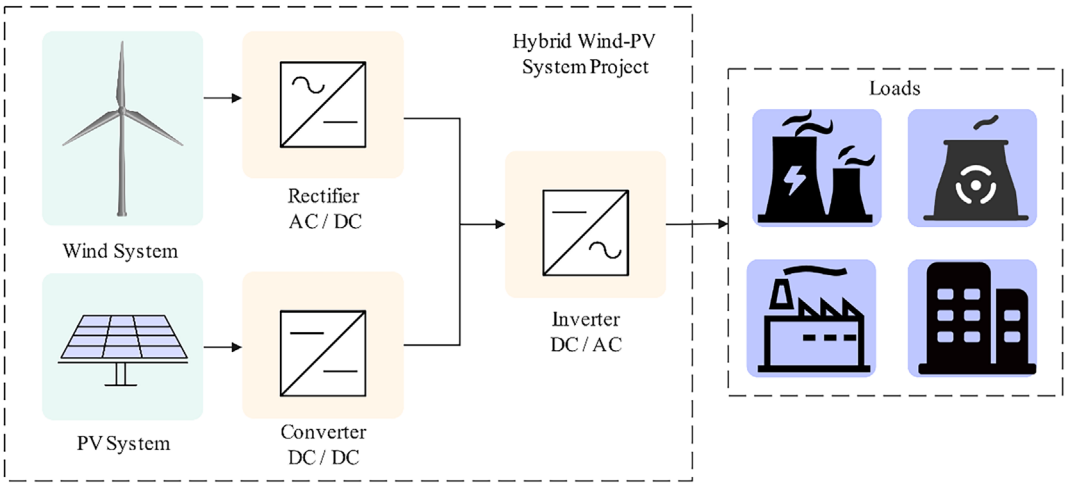

FIG. 1. Hardware structure of the HWPSP.

04 March 2026 02:12:36

Published under an exclusive license by AIP Publishing

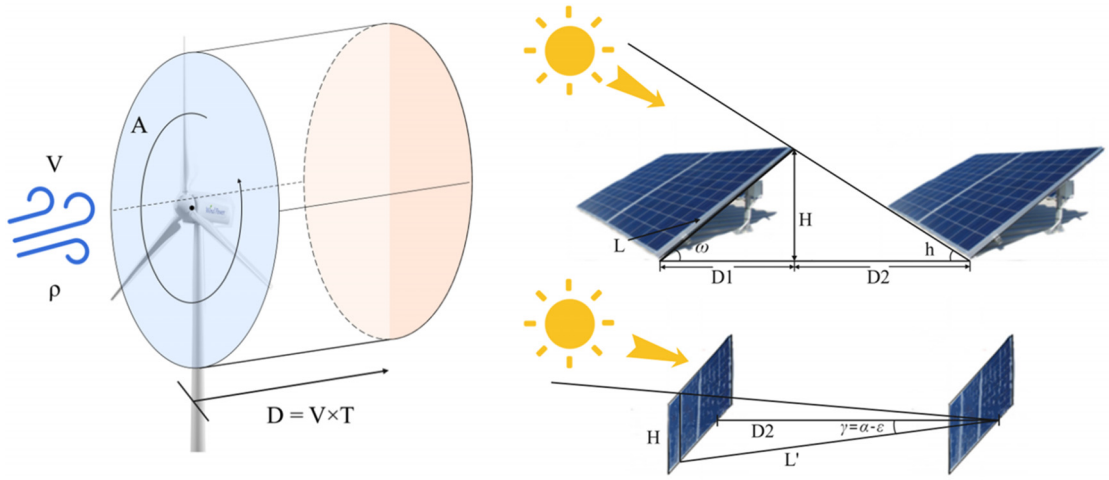

(a) (b)

FIG. 2. Schematic representation of power generation principles in the HWPSP: (a) Wind energy conversion; (b) PV energy conversion.

operational stability. The fundamental equations governing wind power generation are as follows:

$$E = \frac{1}{2}\rho A V^3 \times t, \tag{1}$$

$$P_w = E/t = \frac{1}{2}\rho A V^3, \tag{2}$$

$$P_m = Rs \times T, \tag{3}$$

$$C_P = \frac{P_m}{P_w}, \tag{4}$$

where E represents the kinetic energy of the wind, ρ is the air density, A is the swept area of the wind turbine blades, and V is the wind speed. The time duration is denoted by t, while P_w refers to the wind power density, which indicates the amount of power passing through a unit area per unit time. P_m is the mechanical power generated by the rotor, calculated as the product of rotor speed Rs and torque T. Finally, C_P is the power coefficient, which defines the efficiency of the turbine in converting wind power P_w into mechanical power P_m.

In the HWPSP, the PV subsystem generates electricity by converting solar irradiance into electrical energy through the PV effect. As shown in Fig. 2(b), the proper design of the PV array layout, including the number of array strings N and the inter-column spacing D, is critical to maximizing the energy output while minimizing shading effects between the rows and columns of panels. The electrical performance parameters of the solar cells in each string must be consistent to ensure optimal power generation, and the number of array strings is calculated using Eqs. (5) and (6). The arrangement of the PV array must ensure that there is no shading between panels, either in the north-south or east-west directions, regardless of the time of day or year. For a fixed PV array configuration, the inter-row spacing is calculated based on geometric considerations of the panel's tilt angle ω, the height H, and the projected shadow length L', ensuring that shadows from one row of panels do not affect the next row. This inter-string spacing can be determined by Eq. (7), which takes into account the sun's position throughout the day and the year, as well as the installation angle and the dimensions of the PV modules. The governing equations for determining the number of array strings and the inter-row spacing are as follows:

$$N \cdot V_{\mathrm{dcmax}} \geq V_{\mathrm{oc}} \cdot [1 + (t - 25) \times k_v], \tag{5}$$

$$\frac{V_{mpptmin}}{V_{pm} \cdot [1 - (t' - 25) \cdot k_v']} \leq N \leq \frac{V_{mpptmax}}{[1 - (t - 25) \cdot k_v']}, \tag{6}$$

$$D = D_1 + D_2 = (L \cdot \cos\omega) + \frac{(L \cdot \sin\omega) \cdot \cos(\alpha - \varepsilon)}{\tan\omega}, \tag{7}$$

where N represents the number of strings in the PV array, V_{dcmax} is the maximum allowable DC input voltage for the inverter. The $V_{mpptmax}$ and V_{pptmin} are the maximum and minimum input voltages adjustable by the MPPT technology. The parameters V_{oc} and V_{pm} represent the open-circuit voltage and the nominal output voltage of the solar cells, respectively. k_v and k_v' are the temperature coefficients of the open-circuit voltage and the operating voltage, while t and t' are the operating temperature extremes of the solar cells. The inter-string spacing D is determined based on the panel dimensions, the installation tilt angle ω, the vertical height H, and the shadow length projection L. By accounting for the local climate conditions, including historical temperature extremes, and the technical specifications of the inverter and solar cells, the optimal number of array strings and the appropriate inter-column spacing can be determined, ensuring maximum solar energy capture while avoiding shading effects between rows.

III. INDES EVALUATION SYSTEM

A. Indicator system

The selection of evaluation indicators for the HWPSP assessment system should possess comprehensive, innovative, scientific, and operationally feasible characteristics. This ensures the accuracy of the conclusions drawn from the comprehensive evaluation indicator system

04 March 2026 02:12:36

Published under an exclusive license by AIP Publishing

and provides guiding recommendations for the overall project. The constructed comprehensive evaluation system should maintain good practicality in the future. Therefore, based on the principles mentioned above, the selection of indicators should take into account six major aspects: economic impact, social impact, environmental impact, technical design and equipment selection, natural resource conditions, and CET benefits, as primary indicators (B1-B6). These are further subdivided into 18 secondary indicators related to solar radiation levels, climatic conditions, geological conditions, etc. (C1–C18), as illustrated in Fig. 3.

B. Analysis of the indicator system

1. Natural resources

The evaluation of natural resources for HWPSP involves three main aspects: solar radiation, climatic conditions, and geological conditions. 1. Solar Radiation (C1): Solar radiation is assessed using two factors: monthly average solar radiation and sunlight hours. Data for solar radiation is typically sourced from Meteonorm or PVSYST,[63] while sunlight hours are obtained from local meteorological agencies. These indicators are critical for determining the PV potential of the project and ensuring optimal solar energy capture. 2. Climatic Conditions (C2): Climatic factors impact both wind and PV systems. For wind energy, key metrics include average wind speed, wind direction stability, and the frequency of extreme weather events like storms. For PV systems, parameters such as extreme temperatures, sunny and overcast days, and other weather conditions (e.g., snow or fog) are essential. Combined, these factors ensure that both energy sources operate effectively under diverse weather conditions. 3. Geological Conditions (C3): The evaluation of geological conditions covers topography, geological stability, and hydrology. For wind turbines, stable soil and geological safety are critical for structural integrity, while for PV systems, ground conditions ensure proper installation and minimize hydrological risks. Comprehensive geological assessments support the safe and efficient deployment of both wind and PV components.

By integrating solar, climatic, and geological factors, this evaluation system provides a complete understanding of the site's natural resource potential, ensuring optimal energy generation and long-term operational stability for HWPSP projects.

2. Equipment and technology

The equipment selection for HWPSP is pivotal in ensuring both the efficiency and seamless integration of wind and photovoltaic systems. The following key components are evaluated to guarantee optimal system performance and meet energy demand requirements: 1. Wind Turbine and PV Panel Selection (C4): The choice of wind turbines and photovoltaic (PV) panels is fundamental to the system's capacity to harness renewable energy. Wind turbines must be selected based on parameters such as rotor diameter, hub height, and adaptability to local wind conditions. For PV panels, considerations like conversion efficiency, degradation rate, and performance under diverse sunlight conditions are critical to determining the system's overall energy yield. 2. Rectifier and Converter Selection (C5): The wind energy system requires a rectifier to convert the AC power generated by the wind turbines into DC, while the PV system utilizes a converter to regulate the DC output. The selection of rectifiers and converters should focus on efficiency, operational reliability, and the ability to handle variable power outputs from both wind and solar sources, ensuring seamless integration and minimal energy losses. 3. Inverter Selection (C6): The inverter is responsible for converting DC power from both the wind and PV systems into AC power suitable for grid or load consumption. The inverter selection should prioritize high conversion efficiency, the ability to manage fluctuating power levels, and effective grid synchronization. A reliable inverter ensures stable and high-quality power output for the connected loads. 4. Array Spacing Calculation (C7): Proper spacing of PV arrays is essential to prevent shading and optimize energy capture. The layout must maximize sunlight exposure, while also considering interactions between PV arrays and wind turbines to avoid interference, ensuring efficient land use and optimal system performance. 5. Annual Power Generation

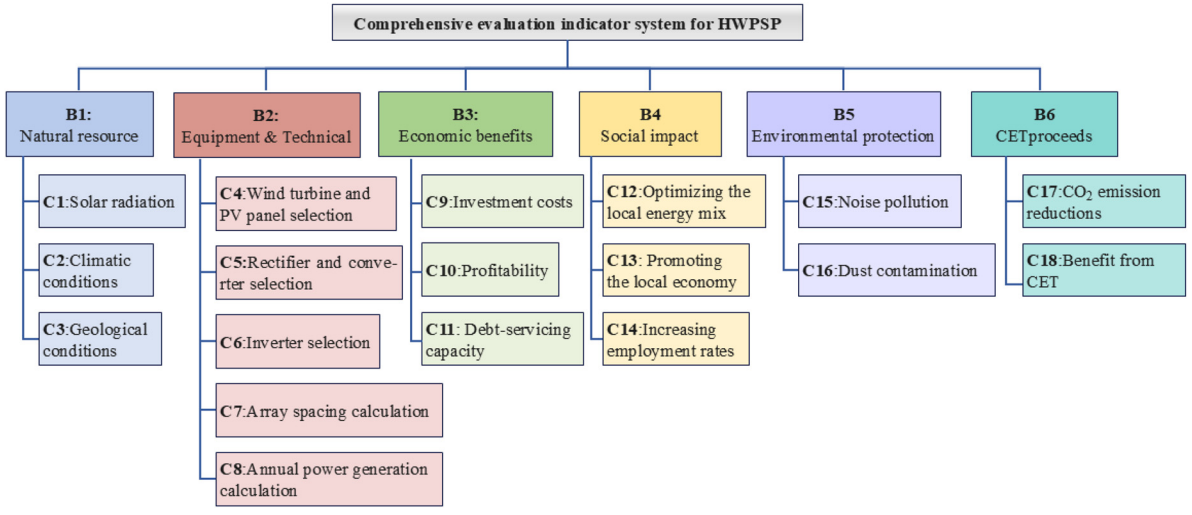

FIG. 3. Comprehensive evaluation indicator system for HWPSP.

04 March 2026 02:12:36

Published under an exclusive license by AIP Publishing

Calculation (C8): Accurately estimating the annual power generation from both the wind and PV systems is critical for evaluating the project's feasibility and long-term performance. This involves modeling expected energy production based on local wind speeds, solar radiation levels, and equipment efficiency. The combined energy output from both systems results in a more stable and reliable energy supply that meets varying load demands. The process for calculating the annual power generation from photovoltaic and wind systems is detailed as follows:

The annual electricity generation of the PV system L_{PV} is calculated using Eqs. (8)–(10)

$$L_{PV} = H_{PV} \times E_{PV}, \tag{8}$$

$$E_{PV} = I_0 \times A_{PV} \times K, \tag{9}$$

$$K = \eta_l \times \eta_i \times \eta_n \times \eta_j \times \eta_q \times \eta_t, \tag{10}$$

where H_{PV} is the annual peak sunshine hours; E_{PV} is the power generated by the PV power generation system; I_0 is the annual solar irradiation;[64] A_{PV} is the mounting area of the PV modules, and K is the integrated efficiency, which accounts for correction factors such as cell type η_l, panel orientation η_i, inverter efficiency η_n, line losses η_j, surface cleanliness η_q, and PV cell conversion efficiency η_t.

For wind power generation, the annual electricity generation considers factors such as air density, turbine utilization rate, and the performance of the power curve. The discount factors include electrical losses from transformers, power collection lines, and environmental effects such as blade soiling and turbulence. The net annual power generation P_n for the wind farm is calculated based on theoretical generation P adjusted by uncertainty and discount factors, as shown in Eqs. (11)–(13)

$$P_n = P_{50} \times (1 - N_v(n\%) \times \sigma), \tag{11}$$

$$P_{50} = P \times D', \tag{12}$$

$$\sigma = \sqrt{\sum_{i=1}^{m} \sigma_i^2}, \tag{13}$$

where P_n is the power generation under the exceeding probability of n%; P_{50} is the net power generation at a 50% probability; $N_v(n\%)$ is a characteristic variable based on standard normal distribution. The certainty discount factor; σ is the total uncertainty, and D' accounts for corrections related to turbine availability, power curve accuracy, electrical efficiency, and environmental impacts.

3. Economic benefits

The economic evaluation of HWPSP takes into account various economic factors, including investment costs, profitability, and debt-servicing capacity. (1) Investment Costs (C9): These encompass expenses related to design, equipment and materials, construction management, and labor. (2) Profitability (C10): The primary source of revenue is the sale of electricity generated by HWPSP at local electricity prices. This involves calculating the total electricity sales revenue and determining the net profit after deducting operational and maintenance costs. (3) Debt-Servicing Capacity (C11): This is assessed through the analysis of net cash flow and the project's payback period, providing insights into the financial stability of the project and its ability to repay investments. These economic indicators are critical for assessing the economic feasibility and long-term sustainability of HWPSP.

4. Social impact

The social impact of HWPSP is assessed through several key indicators, focusing on their contribution to optimizing energy systems, enhancing economic conditions, and supporting societal well-being. 1. Optimizing the Local Energy Mix (C12): HWPSP plays a critical role in balancing and diversifying the local energy supply. By integrating renewable energy sources, these projects contribute to a more sustainable and resilient energy infrastructure, reducing dependency on fossil fuels and enhancing energy security. 2. Promoting the Local Economy (C13): HWPSP can stimulate local economic growth by attracting investments, creating business opportunities, and encouraging the development of green industries. The presence of such projects can foster economic resilience in the community, leading to long-term socioeconomic benefits. 3. Increasing Employment Rates (C14): The construction, operation, and maintenance of HWPSP generate employment opportunities for local residents. This not only provides direct job creation in the renewable energy sector but also supports broader economic development through indirect employment in related industries, such as manufacturing and services. These social impact indicators are crucial for understanding the broader societal benefits that HWPSP will bring to the communities in which they are implemented, supporting the case for increased investment in renewable energy projects.

5. Environmental protection

The environmental protection impact of HWPSP is measured through specific indicators that address the potential environmental concerns associated with these projects, focusing on pollution control and sustainable practices. 1. Noise Pollution (C15): The operation of HWPSP, particularly wind turbines, can generate noise that may affect nearby communities. Evaluating noise pollution involves assessing the sound levels produced during different stages of project operation and implementing noise mitigation measures, such as sound barriers or optimized turbine placement, to minimize the impact on local residents. 2. Dust Contamination (C16): Dust can be generated during the construction phase of HWPSP, as well as from vehicle traffic and material handling. It is important to assess the levels of dust contamination and its potential effects on air quality, especially in areas near residential zones or sensitive ecosystems. Effective dust suppression strategies, such as water spraying and proper site management, are critical to mitigating these environmental impacts. These environmental protection indicators are essential for understanding and addressing the ecological challenges posed by HWPSP, ensuring that these projects not only contribute to energy sustainability but also align with environmental stewardship principles.

6. CET

HWPSP contributes significantly to reducing CO_2 emissions by utilizing clean energy from both wind and solar sources, thus displacing conventional electricity generation and reducing overall CO2 emissions. 1. CO2 Emission Reductions (C16): The carbon emission reduction can be calculated by considering both wind and PV energy

04 March 2026 02:12:36

Published under an exclusive license by AIP Publishing

contributions. Taking the case of a gas-steam combined cycle unit in a power plant as a reference, the steps for calculating carbon dioxide emission reduction for HWPSP are as follows:

$$E_c = EF \times (AD_{PV} + AD_W), \tag{14}$$

$$AD_{PV} = NCV \times FC_{PV}, \tag{15}$$

$$AD_W = NCV \times FC_W, \tag{16}$$

$$EF = CC \times OF \times \frac{44}{12}, \tag{17}$$

$$FC_{PV} = \eta_{PV} \times Q_{PV}, \quad FC_W = \eta_W \times Q_W, \tag{18}$$

where E_c represents the total annual reduction of CO_2 emissions from both PV and wind power. EF is the CO_2 emission factor of natural gas combustion, while AD_{PV} and AD_W denote the annual reductions in energy consumption due to PV and wind power generation, respectively. NCV refers to the net calorific value of the fuel, and FC_{PV} and FC_W are the annual reductions in natural gas consumption attributed to PV and wind energy. CC represents the carbon content of natural gas per unit of calorific value, and OF is the oxygen factor. The ratio of $\frac{44}{12}$ represents the conversion from the atomic mass of carbon to the molecular mass of CO_2; η_{PV} and η_W represent the efficiency of the PV and wind systems, respectively, while Q_{PV} and Q_W refer to the annual energy outputs from the PV and wind systems.

By summing the displaced energy contributions from both PV and wind components, the total CO_2 emission reduction E_c can be calculated. 2. Benefit from CET (C18): The economic benefits of this emission reduction can then be derived by multiplying E_c by the carbon price per unit set by China's carbon trading market for that year. This comprehensive calculation method ensures an accurate reflection of the combined impact of both renewable sources within the HWPSP, providing valuable insights into the project's economic and environmental benefits.

C. Pre-processing of indicators

The evaluation system includes both qualitative and quantitative indicators, and the dimensions of quantitative indicators also vary. Therefore, it is necessary to quantitatively process each indicator in the evaluation system: unify the dimensions of quantitative indicators and quantify qualitative indicators, thereby converting all indicators into specific data reflecting the degree of excellence. This study adopts the expert scoring method, inviting experts in the relevant field to analyze the actual situation of various indicators of HWPSP and assign corresponding scores. The scoring is on a percentage scale, with four levels: excellent, good, medium, and poor. Table II provides the specific scoring criteria:

TABLE II. Criteria for Evaluation of HWPSP.

Levels	Score ranges
Poor	(0,60]
Medium	(60,70]
Good	(70,85]
Excellent	(85,100]

IV. METHOD

A. Weight coefficient calculation

QPSO is employed to optimize the weights in the linear function, establishing a comprehensive evaluation linear weighted function. The optimal weights corresponding to each secondary indicator and the corresponding weights of the primary indicators are obtained. Various secondary indicators Z_1-Z_{18} and their corresponding weight coefficients W_1-W_{18} are selected to calculate the total score Z_t, establishing the corresponding comprehensive evaluation linear weighted functional expression

$$Z_t = W_1 \times Z_1 + W_2 \times Z_2 + \cdots + W_{18} \times Z_{18}. \tag{19}$$

The linear function is optimized using QPSO to determine the optimal weight coefficients W_1–W_{18}, reflecting the comprehensive evaluation of the HWPSP, the position vector of particles is utilized to represent each optimization variable

$$X_i = [W_1 W_2 W_3 \cdots W_{18}]^T. \tag{20}$$

Next, a weight coefficient optimization model is established. The objective function of the design optimization problem and the fitness function of the particle swarm are

$$\mathrm{f}(X_i) = J_i = \frac{\left\| Z_t^0 - Z_t \right\|}{k_z}, \tag{21}$$

where the k_z is the accuracy requirement, J_i is the fitness of the ith particle, Z_t^0 is the evaluation score obtained according to the existing evaluation method, and Z_t is the evaluation score obtained according to Eq. (11). When the fitness $J \leq 1$, it means that the convergence result has met the accuracy requirement of iterative calculation, and each weight coefficient searched can be used as the optimal solution of the weight coefficient optimization problem.

Next, we will enter the optimization process based on QPSO. Let the number of particles in the particle swarm be N, the number of iterative calculations is denoted by t, and the maximum number of iterations is t_{max}. Using the optimization algorithm of quantum particle swarm, the specific process of optimizing the weight coefficients is shown in Fig. 4.

Step 1: Initialize the particle swarm. Set the iteration count t=0, the number of particles N=80, the maximum iteration count t_{max} = 300. Each particle's position vector represents a potential solution for the optimal set of weight coefficients. The dimensionality of the position vector, denoted as M, is equal to the number of weight coefficients, i.e., M = 18. Randomly initialize the initial positions of 80 particles as follows:

$$X_i(0) = [x_{i1} x_{i2} x_{i3} \ldots x_{i18}], \quad i = 1, 2, 3, \ldots, 80. \tag{22}$$

Step 2: Make the local optimal position of each particle $P_i(0) = X_i(0)$, and determine the global optimal position of the particle swarm, i.e., the optimal solution of the weight coefficients $P_g(0)$ is

$$P_g(0) = \min\{X_1(0) X_2(0) X_3(0) \ldots X_N(0)\}. \tag{23}$$

Step 3: Calculate the fitness of each particle. The fitness J_i of each particle is calculated using the adaptation function Eq. (16) established based on the Wind-PV project evaluation criteria.

04 March 2026 02:12:36

Published under an exclusive license by AIP Publishing

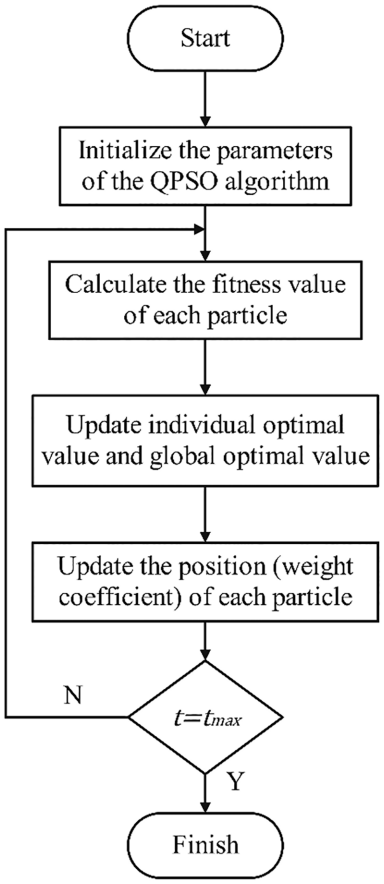

FIG. 4. Flowchart of weight coefficient optimization based on QPSO.

$$f(X_i) = J_i. \tag{24}$$

Step 4: As the iterative computation proceeds, update the new locally optimal position $P_i(t)$ of each particle at the t th iteration to be

$$P_i(t) = \begin{cases} P_i(t-1) & f(P_i(t-1)) < f(X_i) \\ X_i(t) & f(P_i(t-1)) \geq f(X_i). \end{cases} \tag{25}$$

Step 5: Based on the new local optimal position of each particle, update the global optimal position $P_g(t)$ of the particle swarm at the t th iteration, i.e., the optimal weight coefficients are

$$P_g(t) = \min\{P_1(t)P_2(t)\ldots P_N(t)\}. \tag{26}$$

Step 6: Calculate the average optimal position $C(t)$ of the particle swarm at the t th iteration and the random point position p_i of each particle according to Eqs. (27) and (28), and update the new position $X_i(t+1)$ of each particle according to Eq. (29). In the QPSO algorithm, the particle swarm moves the positions of the particles according to Eqs. (27)–(29)

$$P_g(t) = \frac{1}{N}\sum_{i=1}^{N} P_i(t) = \frac{1}{N}\left[\sum_{i=1}^{N} P_{i1}(t), \sum_{i=1}^{N} P_{i2}(t), \ldots, \sum_{i=1}^{N} P_{iM}(t)\right], \tag{27}$$

$$P_{ij}(t) = \varphi_{ij}(t)P_{ij}(t) + \left[1 - \varphi_{ij}(t)\right]P_{gj}(t), \quad j = 1, 2, \ldots, M, \tag{28}$$

$$x_{ij}(t+1) = P_{ij}(t) \pm \alpha(t) \times \left|C_j(t) - x_{ij}(t)\right| \times \ln\left(\frac{1}{u_{ij}(t)}\right), \tag{29}$$

where $P_i(t)$ is the best position vector of the i th particle at the t th iteration; $P_g(t)$ is the global best position vector at the t th iteration; $C(t)$ is the intermediate position vector of the current best positions of all the particles at the t th iteration; $P_i(t)$ is the random position between the best position of the t th particle, $P_i(t)$, and the global best position, $Pg(t)$; $\varphi_{ij}(t+1)$, $u_{ij}(t+1)$ are random numbers obeying uniform distribution on the interval $[0, 1]$.

Step 7: If the termination condition of the algorithm is not satisfied, return to Step 3; otherwise, the algorithm ends. If $t{=}t_{max}$, the algorithm ends.

B. Parameter settings and justification

To ensure the stability and convergence of the QPSO-based weight coefficient optimization model, the key parameters are determined according to established practices in the QPSO literature and preliminary experiments conducted in this study. The contraction-expansion coefficient a(t) is set as a linearly decreasing function, i.e.,

$$\alpha(t) = \alpha_{max} - \frac{t}{t_{max}}(\alpha_{max} - \alpha_{min}), \tag{30}$$

where $\alpha_{max} = 1.0$ and $\alpha_{min} = 0.5$. This setting is widely adopted because a larger $\alpha(t)$ in early iterations promotes global exploration, while a smaller $\alpha(t)$ in later iterations enhances local exploitation, contributing to stable convergence.

The population size $N = 80$ is selected to balance computational efficiency and search diversity. Prior studies indicate that QPSO typically achieves stable convergence with population sizes between 40 and 100; additional experiments in this work showed that increasing the population beyond 80 does not significantly improve performance but increases computation time. The maximum iteration count $t_{max} = 300$ is chosen based on preliminary convergence tests, which indicated that the algorithm consistently converges within 200–250 iterations.

C. Sensitivity analysis of parameter robustness

To verify the robustness of the parameter configuration, sensitivity analyses were performed by varying the population size (40, 60, 80, 100) and the $\alpha(t)$ range (1.2–0.6 and 0.8–0.4). The results show that the ranking outcomes fluctuate by less than 2%, and the fitness curve maintains amonotonic decreasing trend across all settings, demonstrating stable convergence behavior. These findings confirm that the chosen parameter set ($N = 80$, $t_{max} = 300$, $\alpha(t) \in [0.5, 1.0]$) provides a reliable balance between computational cost and solution accuracy.

D. TOPSIS method

After deriving the weights of each indicator based on the above method, the sorting value of each sample can be calculated by the TOPSIS method:

04 March 2026 02:12:36

Published under an exclusive license by AIP Publishing

1. Weighted initial data

According to the comprehensive evaluation system constructed in Sec. III, and according to the following method to derive the weighted indicator matrix

$$R_{ij} = \begin{pmatrix} w_1 \cdot z_{11} & \cdots & w_n \cdot z_{1n} \\ \vdots & \ddots & \vdots \\ w_1 \cdot z_{m1} & \cdots & w_n \cdot z_{mn} \end{pmatrix} = \begin{pmatrix} r_{11} & \cdots & r_{1n} \\ \vdots & \ddots & \vdots \\ r_{m1} & \cdots & r_{mn} \end{pmatrix}, \quad (31)$$

where m represents different comprehensive evaluation results and n is the number of second-level indicators of the comprehensive evaluation system.

2. Calculate positive and negative ideal solutions

The positive ideal solution is the set of maximum values in the weighted comprehensive evaluation indicator matrix, and the negative ideal solution is the set of minimum values in the weighted comprehensive evaluation indicator matrix, and the calculation process is as follows:

$$r_j^* = \max_i r_{ij}, \quad j = 1, 2, \ldots n, \quad (32)$$

$$r_j^0 = \min_i r_{ij}, \quad j = 1, 2, \ldots, n. \quad (33)$$

In the above calculation method, r_j^* represents the positive ideal solution of the weighted indicator matrix, and r_j^0 represents the negative ideal solution of the weighted indicator matrix.

3. Calculation of Euclidean distance

The calculation of the Euclidean distance is based on the following formula

$$s_i^* = \sqrt{\sum_j^n \left(r_{ij} - r_j^*\right)^2}, \quad i = 1, 2, \ldots, m, \quad (34)$$

$$s_i^0 = \sqrt{\sum_j^n \left(r_{ij} - r_j^0\right)^2}, \quad i = 1, 2, \ldots, m. \quad (35)$$

4. Calculation of the final comprehensive evaluation results

By calculating the sorting value f_i^* of each evaluation level, a comprehensive and clear explanation basis can be obtained, which, in turn, leads to the final comprehensive evaluation results, the specific calculation process is as follows:

$$f_i^* = \frac{s_i^0}{\left(s_i^0 + s_i^*\right)}, \quad i = 1, 2, \ldots, m. \quad (36)$$

Through the calculation process described above, the distances between the evaluation rank of each item in the evaluation weighting matrix and the positive and negative ideal solutions can be calculated, and these distances can be expressed in terms of Euclidean distances to map the proximity between the evaluation samples and the ideal situation, i.e., the indicator ranking values. By comparing the ranked values of the indicators and the degree of proximity of each sample to the ideal solution, the best sample can be analyzed.

ALGORITHM 1. QPSO-Based Weight Optimization.

Input: Indicator matrix X, evaluation criteria set C

Output: Optimized weight vector w^*

Initialize population $\{X_i\}$, $i = 1, \ldots, N$
Initialize $\alpha(t)$, maximum iterations T_{max}
Evaluate the fitness of each particle
Set $pbest_i = X_i$ and $gbest = argmax(fitness)$

For $t = 1$ to T_{max} do
    Compute the mean best position: $mbest = \frac{1}{N}\sum_{i=1}^{N} pbest_i$
    for each particle i do
        Generate random numbers $u_1, u_2 \sim U(0, 1)$
        Compute local attractor $P_i = \beta_1 pbest_i + \beta_2 gbest$
        Update position using QPSO update rule:
            $X_i(t+1) = P_i \pm \alpha(t)|mbest - X_i| \cdot \ln\left(\frac{1}{u_1}\right)$
        Evaluate the new fitness of $X_i(t+1)$
        Update $pbest_i$ if improved
    end for
    Update $gbest$ from all $pbest_i$
    Decrease $\alpha(t)$ linearly
end for

return $w^* = gbest$

V. CASE STUDY

A. Scenario description

The proposed comprehensive evaluation system was applied to an HWPSP in Chaoyang District, Beijing, China, associated with a certain thermal power plant. This power plant was chosen for the study due to its location in the north China plain, representing a typical natural environment and sunlight conditions in China. Additionally, the plant is considered relatively typical in terms of its technical scale within China.

The monthly average solar radiation and the average monthly sunshine hours obtained through the Meteonorm program are shown in Fig. 5. The annual average solar total radiation for this power plant is 1385 kWh/m^2.[63] The total electricity generation over the project's entire lifecycle is 30.6641 $\times$ 10^6 kWh, with an annual average electricity generation of 1.227 $\times$ 10^6 kWh. The average annual equivalent utilization hours of the solar panels are 1213.76 h, resulting in an annual reduction in carbon dioxide emissions of approximately 476.72 tons and emission reduction benefits of about 28 000 CNY. The wind power component of the project has a total installed capacity of 100 kW, comprising five 20 kW wind turbines. Based on the average monthly wind speed at the power station from 2012 to 2022, recorded at 11.3 m/s, the average annual power generation is estimated to be 636 000 kWh. Over the entire project cycle, the total power generation is projected to reach 12.72 $\times$ 10^6 kWh. Furthermore, the project is expected to reduce annual carbon dioxide emissions by approximately 247.1 tons, contributing to an emission reduction benefit valued at approximately 14 500 CNY per year.

04 March 2026 02:12:36

Published under an exclusive license by AIP Publishing

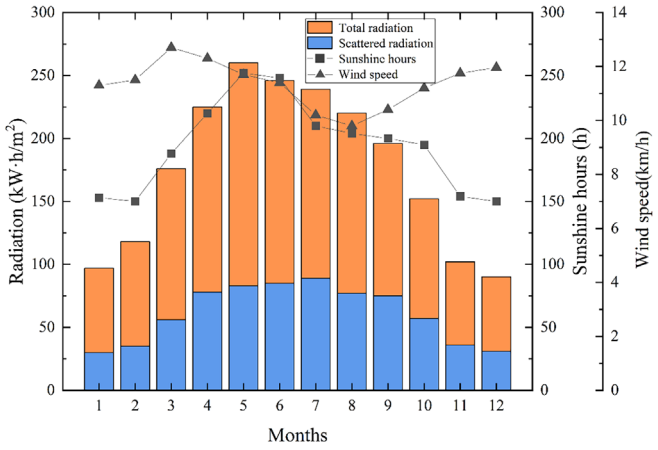

FIG. 5. Average number of hours of sunshine by month at the project site from 2012 to 2022.

To account for the fluctuation of carbon prices in the CET market, a sensitivity analysis was conducted. Based on recent trading data in China's national carbon market, three carbon-price scenarios were considered: Low price: 0.3 CNY/ton (lower-bound fluctuation); Baseline price: 0.56 CNY/ton (current average level); High price: 1.0 CNY/ton (upper-bound stress scenario). For each scenario, the CET-related indicator values were recalculated, and the final project evaluation score was obtained using the proposed QPSO–TOPSIS framework. This setup allows assessing how carbon-price volatility affects the overall evaluation results of hybrid Wind–PV system projects.

B. Indicator calculation results

According to the comprehensive evaluation system for the Wind–PV project, 20 experts from the PV and wind power industry were invited to score the project. The expert group covered diverse professional backgrounds, including renewable energy engineering, power system planning, environmental assessment, and carbon-emission policy, and each expert had more than 10 years of experience. The scoring table was preprocessed into four levels: Excellent, Good, Medium, and Poor. To ensure reliability, all experts scored independently. The consistency of the scoring results was examined using Kendall's W, yielding $W = 0.783$, $p < 0.01$, which indicates a strong level of agreement among experts. All original scores were normalized using the min–max method before constructing the 18×4 indicator evaluation level matrix shown in Fig. 6. Each element in the matrix represents the proportion of expert scores falling into each evaluation level for a specific indicator. For example, for the solar radiation indicator, the value of 0.6 in the "Excellent" category indicates that 12 out of 20 experts assigned a score of 85 or above. A small-sample sensitivity check (randomly removing two experts) caused less than 1.5% variation in aggregated results, confirming the robustness and reproducibility of the expert-based scoring process.

To overcome the limitations of classical optimization algorithms in handling nonlinear and strongly coupled indicators, this study adopts the QPSO method for weight determination. Figure 7 illustrates the convergence behaviors of QPSO and the classical PSO. The results show that the major decrease in fitness for QPSO occurs within the initial iterations, and the algorithm stabilizes after approximately 52 iterations. Under the same parameter settings, classical PSO requires about 81 iterations to reach a comparable level of convergence accuracy, indicating that QPSO achieves an improvement of approximately 35.8% in convergence speed. To further examine the stability of the optimization results, both QPSO and PSO were independently executed 20 times. Their final fitness standard deviations were 0.005 and 0.013, respectively. The significantly lower variance of QPSO demonstrates its superior stability, stronger global convergence capability, and reduced tendency to fall into local optima. The detailed performance comparison is provided in Table III, showing that QPSO consistently

		Excellent	good	medium	poor	Z_t^0
B1	C1	0.6	0.25	0.1	0.05	83.55
	C2	0.4	0.35	0.15	0.1	78.55
	C3	0.45	0.35	0.1	0.1	79.70
	C4	0.5	0.35	0.1	0.05	82.55
B2	C5	0.45	0.25	0.15	0.15	78.45
	C6	0.4	0.3	0.15	0.15	76.95
	C7	0.5	0.25	0.2	0.05	80.20
	C8	0.5	0.25	0.1	0.15	78.15
B3	C9	0.45	0.35	0.15	0.05	79.80
	C10	0.55	0.35	0.05	0.05	84.55
	C11	0.45	0.3	0.2	0.05	79.75
B4	C12	0.45	0.45	0.05	0.05	83.25
	C13	0.45	0.3	0.15	0.1	78.25
	C14	0.2	0.3	0.4	0.1	72.10
B5	C15	0.3	0.45	0.1	0.15	77.25
	C16	0.5	0.25	0.2	0.05	77.85
B6	C17	0.45	0.25	0.15	0.15	78.70
	C18	0.4	0.3	0.15	0.15	77.60

FIG. 6. Indicator evaluation rating matrix.

04 March 2026 02:12:36

Published under an exclusive license by AIP Publishing

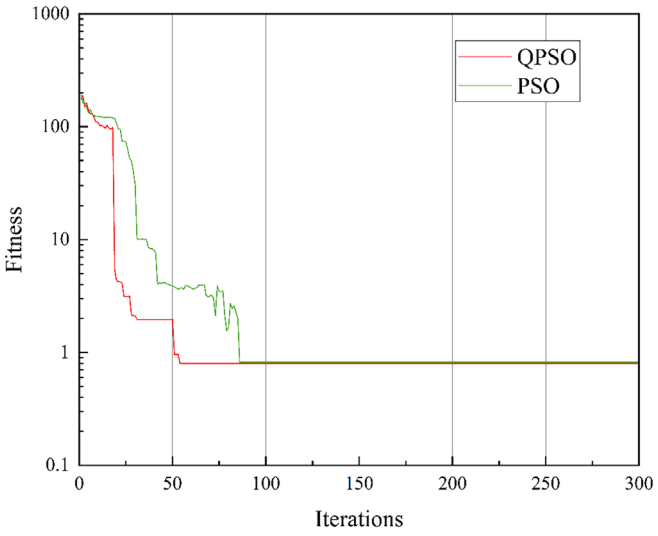

FIG. 7. Iterative optimization process of QPSO.

TABLE III. Comparison of optimization performance between QPSO and PSO.

Metric	QPSO	PSO	Improvement
Convergence iteration	54	86	≈ 37% faster
Final fitness	0.803 09	0.823 09	QPSO better
STD (20 runs)	0.005	0.013	QPSO variance ↓ 61%
Local optimum risk	Low	Medium–High	QPSO more robust
Parameter dependence	Low	Medium	QPSO requires fewer heuristics

outperforms PSO in convergence speed, final fitness, variance across runs, and global search ability.

In addition, Table IV reports the results of the sensitivity analysis conducted under 5%–10% indicator perturbations. The QPSO-TOPSIS model maintains high ranking stability, with variations in relative closeness remaining within ±2% across all perturbation levels. In contrast, traditional linear MCDM methods exhibit fluctuations of 8%–12% and even cause ranking changes in some cases. These findings collectively confirm that the proposed QPSO-enhanced framework not only provides faster and more reliable convergence but also demonstrates significantly stronger robustness against indicator uncertainties.

TABLE IV. Sensitivity analysis under 5%–10% indicator perturbation.

Perturbation level	QPSO score fluctuation	PSO score fluctuation	Ranking stability
5%	±1.2%	±8.5%	QPSO stable; PSO unstable
10%	±1.9%	±11.4%	QPSO stable; PSO ranking changed

TABLE V. Optimization results of weight coefficients of secondary indicators.

Indicator		Value	
B1	C1	0.098	0.191
	C2	0.038	
	C3	0.055	
B2	C4	0.081	0.249
	C5	0.031	
	C6	0.025	
	C7	0.062	
	C8	0.050	
B3	C9	0.063	0.226
	C10	0.109	
	C11	0.054	
B4	C12	0.103	0.175
	C13	0.042	
	C14	0.030	
B5	C15	0.042	0.104
	C16	0.062	
B6	C17	0.031	0.056
	C18	0.025	

The weight distribution in Table V and Fig. 8 reflects the relative importance of each primary indicator within the HWPSP evaluation framework. The environmental indicator (B2) receives the highest weight (0.249), highlighting that environmental performance—such as emission reduction, ecological impacts, and environmental sustainability—is the most critical dimension in evaluating hybrid Wind–PV systems. This outcome is consistent with global renewable energy policies, where carbon mitigation and ecological protection have become central drivers of clean energy project deployment. Experts also emphasized that environmental benefits are increasingly prioritized in regional energy planning, especially under carbon neutrality targets. The economic indicator (B3) ranks second with a weight of 0.226. While economic feasibility remains essential—covering life-cycle cost, capital expenditure, and revenue stability—its slightly lower weight compared with B2 reflects the growing trend in which environmental considerations surpass purely financial factors in renewable energy evaluation. Nonetheless, the high weight of B3 indicates that economic viability continues to play a dominant role in determining project acceptability, particularly in regions with significant initial investment barriers. The natural-resource indicator (B1) follows with a weight of 0.191. The importance of B1 reflects the dependence of HWPSP performance on local wind and solar resource availability. Variability in irradiance and wind speed directly affects power generation stability, making resource endowment a crucial prerequisite for system planning. Sociotechnical (B4, 0.175) and operational indicators (B5, 0.104) receive moderate weights. While factors such as grid-support capability, maintenance difficulty, and social acceptance influence long-term system performance, experts generally view these aspects as supplementary compared with environmental and economic dimensions.

04 March 2026 02:12:36

Published under an exclusive license by AIP Publishing

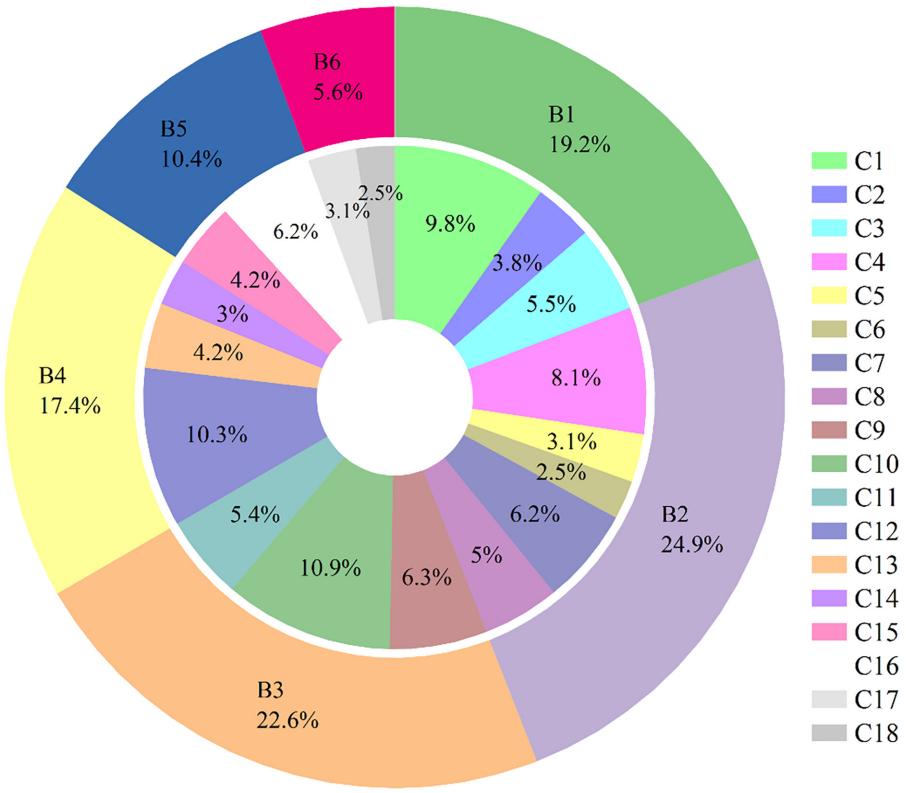

FIG. 8. The percentage of weight values for each indicator.

Finally, the CET-related indicator (B6) receives the lowest weight (0.056). Although carbon-emission trading aligns with long-term environmental strategies, its direct financial influence on HWPSP projects is still limited due to modest carbon price volatility and inconsistent policy incentives. Experts noted that B6 may gain importance as carbon markets mature and stronger policy linkages emerge. Overall, the ranking pattern—Environmental (B2) > Economic (B3) > Natural Resource (B1) > Sociotechnical (B4) > Operational (B5) > CET (B6)—is consistent with expert judgment and reflects the practical priorities observed in HWPSP project assessment.

C. Comprehensive evaluation results

Based on the obtained weight coefficients, a comprehensive evaluation was conducted using the TOPSIS method. The corresponding ideal solution and negative ideal solution, as well as the Euclidean distances between the best and worst solutions, are calculated and presented in Fig. 9 and Table VI, respectively.

Since the elements of the indicator evaluation level matrix represent the proportion of expert evaluations for each indicator level, the optimal solution of the matrix represents the scoring tendency of the majority of experts, while the worst solution represents the scoring tendency of a minority of experts. Therefore, after calculating the Euclidean distance between each evaluation layer and the optimal solution, the worst solution is considered to calculate the ranking value of each evaluation layer. By comparing the Euclidean distances between each evaluation level and the best and worst solutions, it was observed that the results for the Excellent evaluation level have a clear advantage,

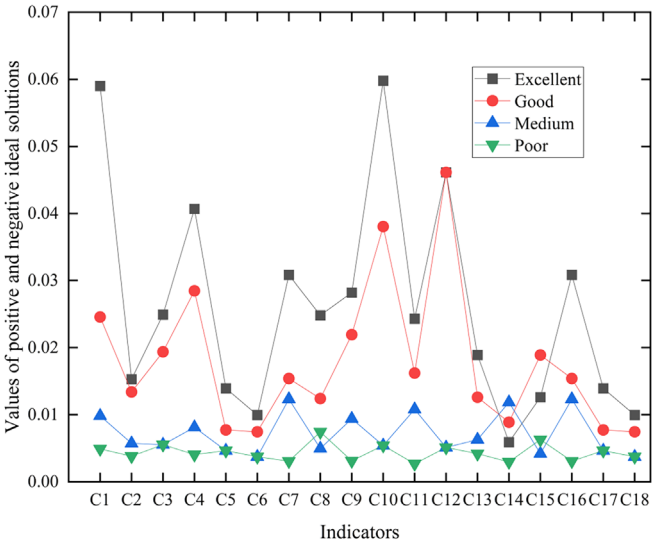

FIG. 9. Weighted indicator evaluation classes and their positive and negative ideal solutions.

with the best ranking value. Therefore, based on the comprehensive considerations, the evaluation level for the HWPSP at a certain thermal power plant is categorized as Excellent, indicating a high-quality project.

04 March 2026 02:12:36

Published under an exclusive license by AIP Publishing

TABLE VI. Euclidean distance of each evaluation class from the optimal and worst solutions.

Evaluation level	With the worst solution	With the optimal solution	Normalized ranking values	Ranking
Excellent	0.409	0.046	0.526	1
Good	0.261	0.189	0.339	2
Medium	0.089	0.369	0.114	3
Poor	0.015	0.412	0.021	4

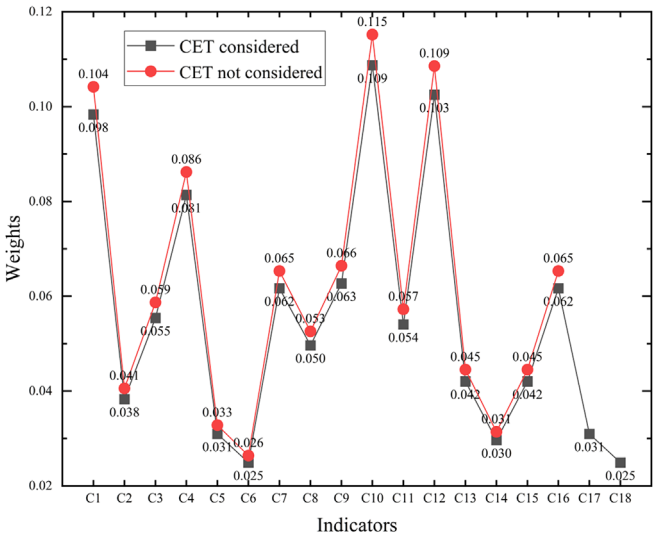

FIG. 10. Comparison of weight values for the indicator system considering CET or not.

D. Comparison experiments

Similarly, we can use the above process to calculate the weights, Euclidean distances, and ranking values of various indicators that do not consider the benefits of CET. The results of the experimental group considering CET were then compared. The comparison of indicator weights for the two scenarios is illustrated in Fig. 10, while the comparative results of Euclidean distances and their ranking values are presented in Table VII.

The inclusion of CET benefits, as evident from Fig. 10, results in a more reasonable distribution of weights in the comprehensive evaluation indicator system. This integration reduces the gap between the weights of advantageous and disadvantageous indicators. The original indicators, including natural resource conditions, equipment technical conditions, project economic benefits, project social impact, and project environmental protection, all exhibit a decreasing trend in weight. The addition of the CET indicator does not alter the original weight ranking of indicators and more accurately reflects the proportion of weights for each indicator. Since the project's capacity is 1.01 MWp, categorized as a small-scale wind-PV facility, the generated carbon dioxide emission reduction is relatively low, and the annual revenue from CET is also modest. Consequently, the weight of the CET indicator is relatively low. Therefore, the thermal power enterprise should consider increasing the scale of the wind-PV project to enhance carbon dioxide emission reduction and revenue from CET, aiming for a higher weight for the CET indicator.

Similarly, by examining the data in Table VII, it is evident that the inclusion of the CET indicator brings the evaluation level of the HWPSP at a certain thermal power plant closer to the excellent solution in terms of Euclidean distance, reducing by approximately 4.17%. Furthermore, the addition of the CET indicator enhances the comprehensive ranking value for the evaluation level classified as excellent, indicating that the inclusion of CET benefits can improve the overall evaluation results for the wind-PV project at the thermal power plant.

E. Carbon price sensitivity analysis

To further examine the robustness of the proposed QPSO–TOPSIS evaluation framework under carbon market uncertainty, a sensitivity analysis was performed using three representative carbon-price levels in China's national CET market: 0.30 CNY/ton (low), 0.56 CNY/ton (baseline), and 1.00 CNY/ton (high). For each scenario, the CET-related indicator value was recalculated, and the overall evaluation score of the wind–PV hybrid project was derived following the same weighting and ranking procedures. The corresponding results are summarized in Table V. The sensitivity results indicate that fluctuations in carbon price lead to measurable yet moderate changes in the final evaluation score. When the carbon price dropped to 0.30 CNY/ton, the comprehensive score decreased by 1.8%. Conversely,

TABLE VII. Comparative table of distances to the optimal solution and evaluation level ranking values.

	Euclidean distance		Normalized ranking values	
Evaluation level	CET considered	CET not considered	CET considered	CET not considered
Excellent	0.046	0.048	0.526	0.524
Good	0.189	0.191	0.339	0.340
Medium	0.369	0.374	0.114	0.115
Poor	0.412	0.419	0.021	0.021

04 March 2026 02:12:36

Published under an exclusive license by AIP Publishing

TABLE VIII. Sensitivity of evaluation score to carbon-price fluctuations.

Scenario	Carbon price (CNY/t)	Evaluation score	Change (%)
Low	0.30	0.835	−1.8%
Baseline	0.56	0.850	0%
High	1.00	0.872	+2.6%

increasing the carbon price to 1.00 CNY/ton resulted in a 2.6% improvement. These variations demonstrate that the economic benefits from carbon emission reduction do influence the evaluation outcome, although the magnitude of the effect remains limited due to the relatively small scale of CO_2 mitigation in the studied wind–PV project. Despite these numerical changes, the ranking order of the evaluation results remained consistent across all carbon-price scenarios, confirming the robustness of the proposed framework. This stability suggests that the multi-indicator decision-making structure, dominated by resource conditions, technical parameters, environmental performance, and economic returns, is resilient to reasonable levels of carbon-price volatility. Nonetheless, the observed score variation highlights that CET-related indicators play a non-negligible role in long-term economic assessments, particularly as China's carbon market continues to expand and carbon prices are expected to rise in the future (Table VIII).

VI. CONCLUSION

This study addresses the challenges posed by evolving carbon market policies and price fluctuations, which complicate the objective evaluation of HWPSPs. To this end, a comprehensive evaluation framework integrating carbon trading mechanisms and quantum optimization is proposed, demonstrating strong potential for practical application. The main conclusions are as follows:

Comprehensive Evaluation Indicator System: A CET-integrated indicator system for HWPSPs was established, fully accounting for the impacts of policy adjustments and carbon price volatility. The proposed indicator system provides a more realistic and rigorous assessment of project feasibility, accurately reflecting the influence of carbon trading policies on renewable energy deployment.

QPSO–TOPSIS Evaluation Method: A quantitative evaluation model combining QPSO with TOPSIS was developed. Leveraging quantum superposition and entanglement within the QPSO optimization process enables the extraction of more reliable and physically grounded weight values for coupled indicators, thereby improving evaluation accuracy compared with traditional linear weighting approaches.

Impact of CET on Evaluation Outcomes: Incorporating CET brings the HWPSP evaluation closer to the ideal scheme, reducing the Euclidean distance by approximately 4.17% and elevating the final ranking to the Excellent level. This demonstrates that CET policies play a meaningful role in improving the attractiveness and investment value of HWPSPs, underscoring the importance of promoting such projects in thermal power plants to support energy conservation, emission reduction, and efficiency improvements.

The conclusions of this study are based on the current impact of CET markets on the operation of power generation enterprises. In the future, various mechanisms such as mandatory carbon reduction, carbon trading, national certification for voluntary emission reduction, and new trading systems are expected to emerge. These developments, along with continued fluctuations in carbon prices, will further affect the operations of power generation enterprises. This research focuses on the analysis of a single HWPSP case, supported by insights from a panel of 20 experts. Future research should aim to expand the sample size to provide more comprehensive and scientifically grounded strategic recommendations for the development of HWPSP.

ACKNOWLEDGMENTS

This work is supported partially by National Natural Science Foundation of China (Grant No. 71974055), 2022 Strategic Research Key Project of Science and Technology Commission of the Ministry of Education, Beijing Science and Technology Project (Z211100004621010), the project of China Three Gorges Corporation named key technologies of intelligent joint regulation and operation with grid connected friendly in power station group of wind, solar photovoltaic and energy storage (WWKY-2021-0173), Huaneng Group Headquarters Science and Technology Project (HNKJ20-H88), 2022 Strategic Research Key Project of Science and Technology Commission of the Ministry of Education, State Key Laboratory of Alternate Electrical Power System with Renewable Energy Sources (Grant No. LAPS25002), Fundamental Research Funds for the Central Universities (2025MS048) and the NCEPU "Double First-Class" Program.

AUTHOR DECLARATIONS

Conflict of Interest

The authors have no conflicts to disclose.

Author Contributions

Zhanpeng Xu and Zhehan Li contributed equally to this work.

Zhanpeng Xu: Data curation (equal); Formal analysis (equal); Funding acquisition (equal); Investigation (equal); Methodology (equal); Project administration (equal); Resources (equal); Software (equal); Supervision (equal); Validation (equal); Visualization (equal); Writing – original draft (equal); Writing – review & editing (equal). **Zhehan Li:** Conceptualization (equal); Data curation (equal); Formal analysis (equal); Funding acquisition (equal); Investigation (equal); Methodology (equal); Project administration (equal); Resources (equal); Software (equal); Supervision (equal); Validation (equal); Visualization (equal); Writing – original draft (equal); Writing – review & editing (equal). **Longze Wang:** Investigation (equal); Supervision (equal); Validation (equal); Writing – review & editing (equal). **Shizhao Wang:** Conceptualization (equal); Data curation (equal); Formal analysis (equal); Funding acquisition (equal); Investigation (equal); Methodology (equal); Project administration (equal); Resources (equal); Software (equal); Supervision (equal); Validation (equal); Visualization (equal); Writing – original draft (equal); Writing – review & editing (equal). **Yuteng Mao:** Conceptualization (equal); Data curation (equal); Formal analysis (equal); Funding acquisition (equal); Investigation (equal); Methodology (equal); Project administration (equal); Resources (equal); Software (equal); Supervision (equal); Validation (equal); Visualization (equal); Writing – original draft (equal); Writing – review & editing (equal). **Zhenhao Weng:** Conceptualization (equal); Data curation (equal); Formal analysis (equal); Funding acquisition (equal); Investigation (equal); Methodology (equal); Project administration (equal); Resources (equal); Software (equal); Supervision (equal); Validation (equal); Visualization (equal); Writing – original draft

04 March 2026 02:12:36

Published under an exclusive license by AIP Publishing

(equal); Writing – review & editing (equal). **Yan Zhang:** Conceptualization (equal); Data curation (equal); Formal analysis (equal); Funding acquisition (equal); Investigation (equal); Methodology (equal); Project administration (equal); Resources (equal); Software (equal); Supervision (equal); Validation (equal); Visualization (equal); Writing – original draft (equal); Writing – review & editing (equal). **Zihan Xie:** Conceptualization (equal); Data curation (equal); Formal analysis (equal); Funding acquisition (equal); Investigation (equal); Methodology (equal); Project administration (equal); Resources (equal); Software (equal); Supervision (equal); Validation (equal); Visualization (equal); Writing – original draft (equal); Writing – review & editing (equal). **Meicheng Li:** Conceptualization (equal); Data curation (equal); Formal analysis (equal); Funding acquisition (equal); Investigation (equal); Methodology (equal); Project administration (equal); Resources (equal); Software (equal); Supervision (equal); Validation (equal); Visualization (equal); Writing – original draft (equal); Writing – review & editing (equal).

DATA AVAILABILITY

The data that support the findings of this study are available from the corresponding author upon reasonable request.

NOMENCLATURE

AHP	Analytic hierarchy process
CET	Carbon emission trading
CO_2	Carbon dioxide
COPRAS	Complex proportional assessment
DEA	Data envelopment analysis
GDP	Gross domestic product
HWPSP	Hybrid wind–photovoltaic system project
LEC	Life cycle cost
MCDM	Multi-criteria decision making
NO_x	Nitrogen oxides
PSO	Particle swarm optimization
PV	Photovoltaic
QBEA	Quantum-behaved evolutionary algorithm
QGA	Quantum genetic algorithm
QPSO	Quantum particle swarm optimization
SO_2	Sulphur dioxide
TOPSIS	Technique for order preference by similarity to ideal solution
TWh	Terawatt-hour
WT	Wind turbine

APPENDIX A

		Items	Values
Natural resources		Average annual temperature	10–12 °C
		Annual maximum temperature	42 °C
		Annual minimum temperature	−15.5 °C
		Average annual rainfall	600 mm
		Frost-free period of the year	180–220 days
		Annual sunshine hours	2700 h
		Annual number of thunderstorm days	22 days
Equipment and technology	Wind turbine and PV panel selection	Peak power	540 Wp
		open circuit voltage	49.5 V
		short-circuit current	13.9 A
		Operating voltage	41.6 V
		Operating current	13.27 A
		Peak power temperature coefficient	−0.36%/K
		Temperature coefficient of open circuit voltage	−0.28%/K
		Temperature coefficient of short-circuit current	0.048%/K
		10-year power decay	<10%
		25 years of power degradation	<20%
		Module conversion efficiency	20.94%
		Installation size	2274 × 1134 × 35 mm^3
		Weights	28 kg
	Rectifier and converter selection	Power	110 kW
		Types	Stranded
	Inverter	Maximum direct charging input voltage	1100 V
		MPPT voltage range	200–1000 V

04 March 2026 02:12:36

Published under an exclusive license by AIP Publishing

APPENDIX A: (*Continued.*)

		Items	Values
	Array spacing calculation	Component contains	18
		Module power	540 Wp
		Operation mode	fixed tilt
		Tilt angle	36°
		Spacing between front and rear rows	11.7 m
	Annual power generation calculation	Total power generation efficiency	83.31%
		Total power generation in the first year	1 342 409.6 kwh
		Equivalent annual utilization hours	1327.96 h
		The service life of the PERT module	25 years
		Solar module output power decay first year	≤2.0%
		Solar module output power decay (non-first year)	0.55% (linear decay)
		Total power of solar module after 25 years	≥84.8%
		Total power generation over the whole life cycle	30 664 100 kWh
		Average annual power generation	1 227 000 kWh
		Average annual equivalent utilization hours	1213.76 h
Economic benefits		Total project cost	4 257 700 CNY
		Total power after 25 years	≥84.8%
		Average annual power generation over 25 years	1 227 000 kWh
		Total power generation over 25 years	30 674 100 kWh
		Average annual equivalent utilization hours over 25 years	1213.76 h
		Annual generation revenue	300 000 CNY
		Total power generation revenue for the 25-year project	7 930 000 CNY
Social impact of the project		Number of design participants	7
		Number of foundation construction workers	20
		Number of electricians and welders	7
		Number of project managers and equipment manufacturers' supervision engineers	3
		Total jobs provided	37
Environmental protection of the project		Earthmoving noise maximum	70/0 db (day/night)
		Piling noise maximum	70/0 db (day/night)
		Maximum structural noise	70/0 db (day/night)
		Maximum decoration noise	70/0 db (day/night)
CET		Unit type	Gas turbine combined cycle units
		Unit fuel type	petroleum
		Natural gas carbon content per unit calorific value	15.3×10^{-3} tC/GJ
		Fuel carbonization rate	99%
		Comprehensive power supply gas consumption rate	0.1763 m^3/kwh
		The calorific value of natural gas	389.31 GJ/104 Nm^3
		CET market unit price	58.5 CNY/ton

04 March 2026 02:12:36

Published under an exclusive license by AIP Publishing

APPENDIX B

	Project Manager 1	Project Manager 2	Project Manager 3	Project Manager 4	Project Manager 5	Design Unit Engineer 1	Design Unit Engineer 2	Design Unit Engineer 3	Design Unit Engineer 4	Design Unit Engineer 5
C1	83	85	56	66	75	91	86	89	93	94
C2	67	77	69	49	86	85	83	90	82	76
C3	63	51	83	65	86	81	91	82	92	93
C4	80	91	88	82	99	80	59	91	86	90
C5	99	86	93	94	90	67	56	83	43	83
C6	85	83	88	92	90	81	67	55	76	67
C7	90	66	91	92	98	70	69	52	67	86
C8	76	91	86	85	81	86	59	67	46	94
C9	90	86	92	90	80	81	85	79	82	93
C10	90	81	76	83	92	86	63	52	96	86
C11	77	92	90	93	94	90	54	66	63	79
C12	70	72	81	90	83	91	66	69	95	90
C13	86	83	76	92	90	82	39	76	55	83
C14	79	44	81	49	91	83	63	61	67	92
C15	60	51	50	55	61	91	82	83	70	100
C16	89	66	65	41	79	90	86	69	56	55
C17	59	55	83	52	69	93	85	86	90	91
C18	79	56	90	80	91	93	86	83	92	91

	Equipment Manufacturer's Engineer 1	Equipment Manufacturer's Engineer 2	Equipment Manufacturer's Engineer 3	Equipment Manufacturer's Engineer 4	Equipment Manufacturer's Engineer 5	Offeror s Project Manager 1	Offerors Project Manager 2	Offerors Project Manager 3	Offerors Project Manager 4	Offerors Project Manager 5
C1	94	80	96	85	93	83	90	67	79	86
C2	75	89	89	63	95	89	79	73	90	65
C3	59	86	85	80	89	72	73	94	90	79
C4	76	67	85	69	81	86	89	80	82	90
C5	80	69	91	72	92	62	55	86	91	77
C6	69	50	90	55	86	79	82	83	75	86
C7	93	85	79	63	83	91	76	87	90	76
C8	79	45	90	69	86	90	85	83	76	89
C9	90	76	79	67	77	90	66	65	89	39
C10	95	86	92	72	99	83	97	79	100	83
C11	76	64	83	69	83	86	85	75	90	86
C12	92	86	94	80	93	79	82	83	89	80
C13	92	77	86	61	90	63	85	69	91	89
C14	76	65	77	63	93	61	82	60	86	69
C15	89	79	91	82	97	77	82	76	90	79
C16	89	82	93	83	95	96	86	76	91	70
C17	79	81	90	82	69	83	86	86	66	89
C18	79	63	83	55	89	49	82	60	85	66

Journal of Renewable and Sustainable Energy ARTICLE pubs.aip.org/aip/rse
04 March 2026 02:12:36

REFERENCES

[1]L. Tian, Y. Huang, S. Liu *et al.*, "Application of photovoltaic power generation in rail transit power supply system under the background of energy low carbon transformation," Alexandria Eng. J. **60**(6), 5167–5174 (2021).

[2]S. Dale, *BP Statistical Review of World Energy* (BP PLC, London, UK, 2021), pp. 14–16.

[3]N. Mousavi, M. Mohebbi, and M. Teimouri, "Identifying the most applicable renewable energy systems of Iran," Int. J. Sci. Technol. Res. **6**(30), 51–59 (2017).

[4]K. Ullah, M. A. Tunio, Z. Ullah *et al.*, "Ancillary services from wind and solar energy in modern power grids: A comprehensive review and simulation study," J. Renewable Sustainable Energy **16**(3), 032701 (2024).

[5]Z. Liu, Z. Deng, G. He *et al.*, "Challenges and opportunities for carbon neutrality in China," Nat. Rev. Earth Environ. **3**(2), 141–155 (2021).

[6]L. Wang, S. Jiao, Y. Xie *et al.*, "Two-way dynamic pricing mechanism of hydrogen filling stations in electric-hydrogen coupling system enhanced by blockchain," Energy **239**, 122194 (2022).

[7]Z. Xin-Gang, F. Tian-Tian, M. Yu *et al.*, "Analysis on investment strategies in China: The case of biomass direct combustion power generation sector," Renewable Sustainable Energy Rev. **42**, 760–772 (2015).

[8]Z. Peng, X. Chen, and L. Yao, "Research status and future of hydro-related sustainable complementary multi-energy power generation," Sustainable Futures **3**, 100042 (2021).

[9]X. Liu and Y. Long, "Impact of renewable energy intermittency and carbon tax on investment strategy for grid-connected microgrid in China," J. Renewable Sustainable Energy **17**(1), 015909 (2025).

[10]M. M. Akrofi, M. Okitasari, and R. Kandpal, "Recent trends on the linkages between energy, SDGs and the Paris Agreement: A review of policy-based studies," Discover Sustainability **3**(1), 32 (2022).

[11]B. Tang, X. Fan, Y. Chen *et al.*, "Green certificates—Trends in energy mix development in electricity markets: The case of China," J. Renewable Sustainable Energy **17**(1), 015907 (2025).

[12]Y.-Y. Chi, H. Zhao, Y. Hu *et al.*, "The impact of allocation methods on carbon emission trading under electricity marketization reform in China: A system dynamics analysis," Energy **259**, 125034 (2022).

[13]M. Shi, T. Zou, J. Xu *et al.*, "Can carbon emissions trading scheme make power plants greener? Firm-level evidence from China," Front. Energy Res. **10**, 906033 (2022).

[14]G. Yenig and M. Çağlar *et al.*, "On the modeling of CO_2 EUA and CER Prices of EU-ETS for the 2008–2012 period," Appl. Stochastic Models Bus. Ind. **32**(4), 375–395 (2016).

[15]C. Gavard and D. Kirat, "Flexibility in the market for international carbon credits and price dynamics difference with European allowances," Energy Econ. **76**, 504–518 (2018).

[16]G. S. Atsalakis, "Using computational intelligence to forecast carbon prices," Appl. Soft Comput. **43**, 107–116 (2016).

[17]J. Morris, S. Paltsev, and A. Y. Ku, "Impacts of China's emissions trading schemes on deployment of power generation with carbon capture and storage," Energy Econ. **81**, 848–858 (2019).

[18]L. Wang, Y. Zhang, Z. Li *et al.*, "P2P trading mode for real-time coupled electricity and carbon markets based on a new indicator green energy," Energy **285**, 129179 (2023).

[19]Z. Xin-Gang and W. Zhen, "Carbon emission reduction effect of China's low-carbon energy transition policy: An empirical analysis based on policy quantification," J. Renewable Sustainable Energy **15**(1), 015901 (2023).

[20]M. I. Khan, F. Asfand, and S. G. Al-Ghamdi, "Progress in research and technological advancements of commercial concentrated solar thermal power plants," Sol. Energy **249**, 183–226 (2023).

[21]C. Yang, Q. Jiang, Y. Cui *et al.*, "Photovoltaic project investment based on the real options method: An analysis of the East China power grid region," Utilities Policy **80**, 101473 (2023).

[22]S. Zhao, L. Yu, and Z. Zhang, "Photovoltaic supply chain and government subsidy decision-making based on China's industrial distributed photovoltaic policy: A power perspective," J. Cleaner Prod. **413**, 137438 (2023).

[23]L. Liu, Z. Wang, Y. Wang *et al.*, "Optimizing wind/solar combinations at finer scales to mitigate renewable energy variability in China," Renewable Sustainable Energy Rev. **132**, 110151 (2020).

[24]H. Xu, R. Dong, Y. Cui *et al.*, "Does the photovoltaic poverty alleviation project promote county economic development?: Evidence from 852 counties in China," Sol. Energy **248**, 51–63 (2022).

[25]J. Gao, Y. Wang, N. Huang *et al.*, "Optimal site selection study of wind-photovoltaic-shared energy storage power stations based on GIS and multi-criteria decision making: A two-stage framework," Renewable Energy **201**, 1139–1162 (2022).

[26]S. Gökmener, E. Oğuz, M. Deveci, and K. Göllü, "Site selection for floating photovoltaic system on dam reservoirs using sine trigonometric decision making model," Ocean Eng. **281**, 114820 (2023).

[27]A. Alharbi, Z. Awwad, A. Habib *et al.*, "Economical sizing and multi-azimuth layout optimization of grid-connected rooftop photovoltaic systems using mixed-integer programming," Appl. Eng. **335**, 120654 (2023).

[28]A. Barbón, M. Ghodbane, L. Bayón, and Z. Said, "A general algorithm for the optimization of photovoltaic modules layout on irregular rooftop shapes," J. Cleaner Prod. **365**, 132774 (2022).

[29]C. Ghenai, M. A. Rasheed, M. J. Alshamsi *et al.*, "Design of hybrid solar photovoltaics/shrouded wind turbine power system for thermal pyrolysis of plastic waste," Case Stud. Therm. Eng. **22**, 100773 (2020).

[30]E. Yin and Q. Li, "Achieving extensive lossless coupling of photovoltaic and thermoelectric devices through parallel connection," Renewable Energy **193**, 565–575 (2022).

[31]G. N. D. De Doile, P. R. Junior, L. C. S. Rocha *et al.*, "Impacts of economic regulation on photovoltaic distributed generation with battery energy storage systems," J. Energy Storage **72**, 108382 (2023).

[32]A. Burgio, D. Cimmino, M. Dolatabadi *et al.*, "Virtual energy storage system for peak shaving and power balancing the generation of a MW photovoltaic plant," J. Energy Storage **71**, 108204 (2023).

[33]U. G. Onu, G. S. Silva, A. C. Z. de Souza, B. D. Bonatto *et al.*, "Integrated design of photovoltaic power generation plant with pumped hydro storage system and irrigation facility at the Uhuelem-Amoncha African community," Renewable Energy **198**, 1021–1031 (2022).

[34]L. Wang, S. Jiang, Y. Shi *et al.*, "Blockchain-based dynamic energy management mode for distributed energy system with high penetration of renewable energy," Int. J. Electr. Power Energy Syst. **148**, 108933 (2023).

[35]M. Afridi, S. Tatapudi, J. Flicker *et al.*, "Reliability evaluation of DC power optimizers for photovoltaic systems: Accelerated testing at high temperatures with fixed and cyclic power stresses," Eng. Failure Anal. **152**, 107484 (2023).

[36]A. Azzam, M. El Zayat, and M. Marzouk, "Integrated approach for sustainability assessment in power plant projects using building information modeling," Energy Sustainable Dev. **66**, 222–237 (2022).

[37]J. Li, F. Xiong, M. Fan *et al.*, "The role of nonfood bioethanol production in neutralizing China's transport carbon emissions: An integrated life cycle environmental-economic assessment," Energy Sustainable Dev. **70**, 68–77 (2022).

[38]X. Guo, Y. Sun, and D. Ren, "Life cycle carbon emission and cost-effectiveness analysis of electric vehicles in China," Energy Sustainable Dev. **72**, 1–10 (2023).

[39]O. Lyulyov, I. Vakulenko, T. Pimonenko *et al.*, "Comprehensive assessment of smart grids: Is there a universal approach?" Energies **14**(12), 3497 (2021).

[40]A. Makarov, F. Veselov, A. Makarova *et al.*, "Comprehensive assessment of Russia's electric power industry's technological transformation," Therm. Eng. **66**, 687–701 (2019).

[41]B. Shi and H. Wang, "Policy effectiveness and environmental policy Assessment: A model of the environmental benefits of renewable energy for sustainable development," Sustainable Energy Technol. Assess. **57**, 103153 (2023).

[42]Y. Guan, Z. Liu, Y. Du *et al.*, "Evaluating batteries for renewable energy storage: A hybrid MCDM framework based on combined objective weights and uncertainty-preserved COPRAS," J. Renewable Sustainable Energy **15**(4), 044102 (2023).

[43]A. Gupta and S. Suhag, "Evaluation of energy storage systems for sustainable development of renewable energy systems—A comprehensive review," J. Renewable Sustainable Energy **14**(3), 032702 (2022).

[44]Ü. Ağbulut, G. Yildiz, H. Bakir *et al.*, "Current practices, potentials, challenges, future opportunities, environmental and economic assumptions for Türkiye's clean and sustainable energy policy: A comprehensive assessment," Sustainable Energy Technol. Assess. **56**, 103019 (2023).

[45]R. P. Feynman, "Simulating physics with computers," Int. J. Theor. Phys. **21**(6/7), 467 (1982).

04 March 2026 02:12:36

Published under an exclusive license by AIP Publishing

[46]P. W. Shor, "Algorithms for quantum computation: Discrete logarithms and factoring," in *Proceedings of the 35th Annual Symposium on Foundations of Computer Science*, 1994.
[47]L. K. Grover, "A fast quantum mechanical algorithm for database search," in *Proceedings of the Twenty-Eighth Annual ACM Symposium on Theory of Computing*, 1996.
[48]U. Roy, S. Roy, and S. Nayek, "Optimization with quantum genetic algorithm," Int. J. Comput. Appl. **102**(16), 1–7 (2014).
[49]K. H. Han and J. H. Kim, "Genetic quantum algorithm and its application to combinatorial optimization problem," in *Proceedings of the 2000 Congress on Evolutionary Computation CEC00* (IEEE, 2000), Cat No 00TH8512.
[50]P. Li and S. Li, "Quantum ant colony algorithm for continuous space optimization," Control Theory Appl. **25**(2), 237–241 (2008).
[51]J. Sun, W. Xu, W. Fang *et al.*, "Quantum-behaved particle swarm optimization with binary encoding," in *Proceedings of the Adaptive and Natural Computing Algorithms: 8th International Conference (ICANNGA 2007)*, Warsaw, Poland, April 11–14 (Springer, 2007), Part I 8.
[52]H. Gao, Y. Liu, and M. Diao, "Robust multi-user detection based on quantum bee colony optimisation," Int. J. Innovative Comput. Appl. **3**(3), 160–168 (2011).
[53]A. Layeb, "A novel quantum-inspired cuckoo search for knapsack problems," Int. J. Bio-Inspired Comput. **3**(5), 297–305 (2011).
[54]B. B. Maaroof, T. A. Rashid, J. M. Abdulla *et al.*, "Current studies and applications of shuffled frog leaping algorithm: A review," Arch. Comput. Methods Eng. **29**(1), 3459–3474 (2022).
[55]A. Choudhury, S. Samanta, S. Pratihar *et al.*, "Multilevel segmentation of Hippocampus images using global steered quantum inspired firefly algorithm," Appl. Intell. **52**(7), 7339–7372 (2022).
[56]X.-S. Yang and X. He, "Bat algorithm: Literature review and applications," Int. J. Bio-Inspired Comput. **5**(3), 141–149 (2013).
[57]X. Xu, D. Shan, G. Wang *et al.*, "Multimodal medical image fusion using PCNN optimized by the QPSO algorithm," Appl. Soft Comput. **46**, 588–595 (2016).
[58]T. Liu, Z. Ren, C. Xiong *et al.*, "Optoacoustic classification of diabetes mellitus with the synthetic impacts via optimized neural networks," Heliyon **9**(10), e20796 (2023).
[59]G. Qin, A. Xia, H. Lu *et al.*, "A hybrid machine learning model for predicting crater width formed by explosions of natural gas pipelines," J. Loss Prev. Process Ind. **82**, 104994 (2023).
[60]Y. Bai, C. Zhang, Z. He *et al.*, "Inverse solution to two-dimensional transient coupled radiation and conduction problems and the application in recovering radiative thermo-physical properties of Si_3N_4 ceramics," Int. J. Therm. Sci. **190**, 108303 (2023).
[61]M. Tawalbeh, A. Farooq, R. Martis *et al.*, "Optimization techniques for electrochemical devices for hydrogen production and energy storage applications," Int. J. Hydrogen Energy **52**, 1058–1092 (2023).
[62]Z. Cai, Y. Liu, X. Liu *et al.*, "Prediction of interference current of buried pipeline and study on corrosion of Q235A steel," Constr. Build. Mater. **400**, 132739 (2023).
[63]X. Meng, Y. Liu, Y. Han *et al.*, "Defining and grading passive solar heating potential indicator in China: A new irradiation degree hour ratio parameter," Sol. Energy **252**, 342–355 (2023).
[64]M. Mahzarnia, M. P. Moghaddam, P. Siano *et al.*, "A comprehensive assessment of power system resilience to a hurricane using a two-stage analytical approach incorporating risk-based index," Sustainable Energy Technol. Assess. **42**, 100831 (2020).

04 March 2026 02:12:36

Published under an exclusive license by AIP Publishing